Binding of Calcium and Phosphate Ions to Dentin Phosphophoryn†

Mary E. Marsh
Dental Science Institute, The University of Texas Health Science Center, Houston, Texas 77225
Received May 23, 1988; Revised Manuscript Received August 16, 1988

ABSTRACT: The concomitant binding of calcium and inorganic phosphate ions by the highly phosphorylated rat dentin phosphophoryn (HP) was measured in the pH range of 7.4–8.5 by an ultrafiltration procedure. HP binds almost exclusively the triply charged PO_4^{3-} ion, and for each PO_4^{3-} ion bound, the protein binds about 1.5 additional Ca^{2+} ions. Therefore, the protein–mineral ion complex can be described as a protein with two different ligands, Ca^{2+} ions and calcium phosphate clusters having a stoichiometry of about $Ca_{1.5}PO_4$. Empirically the binding of calcium and phosphate can best be described as a function of a neutral ion activity product in which 2.5–10% of the phosphate is HPO_4^{2-}. The stoichiometry of the bound clusters is similar to that of amorphous calcium phosphate, and it is clear that the protein does not sequester crystal embryos of octacalcium phosphate or hydroxyapatite. The protein–mineral ion complex is amorphous by electron diffraction analysis and does not catalyze the formation of a crystalline phase when aged in contact with its solution. About 15% of the bound phosphate is buried in protected domains, and it is stable with respect to dissociation for extended periods in phosphate-free calcium buffers. The buried mineral maintains the protein in an aggregated state even at calcium ion concentrations which are too low for the aggregation of unmineralized HP. In vivo HP should be ineffective in the nucleation of a crystalline mineral phase, if it is secreted in a mineralized aggregated state similar to casein and the bivalve phosphoprotein.

Phosphophoryn is a high-capacity calcium-binding protein, and it is the major noncollagenous protein of rat incisor dentin (Lee et al., 1977; Linde et al., 1980). Consistent with these characteristics, phosphophoryn is a postulated intermediate in dentin mineralization (Veis, 1978; Glimcher, 1981). Because the interaction of phosphophoryn with calcium phosphate, collagen, and the noncollagenous proteins of dentin is poorly understood, the role of phosphophoryn in the mineralization process is undefined. Phosphophoryn may influence the crystallization of dentin calcium phosphate. In vitro the protein inhibits the conversion of amorphous calcium phosphate (ACP)[1] to hydroxyapatite (HA) in synthetic extracellular fluids (Termine & Conn, 1976; Termine et al., 1980). At higher calcium phosphate products and low protein concentration, phosphophoryn catalyzes the crystallization of HA (Nawrot et al., 1976). Phosphophoryn may also function as an intermediate calcium carrier. In vivo a portion of the phosphophoryn secreted by the rat odontoblasts may be turned over; if so, the degraded protein could release mineral ions for crystal growth (Dimuzio & Veis, 1978; Maier et al., 1983).

Theoretical models predict that calcium–protein complexes promote mineralization by binding or attracting a local concentration of anions capable of forming ion pairs with calcium (Crenshaw, 1982; Glimcher, 1981). Further accretion of calcium ions, anions, and ion pairs results in the deposition and growth of a mineral phase. In support of this theory, calcium phosphate–phosphophoryn complexes have been detected in solution by ^{31}P nuclear magnetic resonance spectroscopy (Lee et al., 1983), and phosphoryn binds to hydroxyapatite with high affinity (Nawrot et al., 1976). However, proteins known to sequester calcium and phosphate ions in vivo (i.e., casein micelles and bivalve phosphoprotein particles) are intermediate calcium carriers and are not involved in the nucleation or growth of a calcium phosphate mineral phase (Marsh, 1988). In casein and the bivalve phosphoprotein, calcium phosphate is buried in protected domains and is not in equilibrium with the free ions of the medium (Marsh & Sass, 1984; Holt, 1982).

In this study, the interaction of calcium and phosphate ions with phosphophoryn was examined on a quantitative basis, to determine whether or not there is a physical basis for postulating a catalytic role for phosphophoryn in the nucleation of dentin HA. The phosphophoryn–mineral ion complex can be described as a protein with two different ligands, Ca^{2+} ions and calcium phosphate clusters having a stoichiometry of about $Ca_{1.5}PO_4$. The protein–mineral ion complex is amorphous by electron diffraction analysis, and it does not promote the nucleation of a crystalline mineral phase. As much as 15% of the sequestered phosphate ions are buried in protected domains.

Materials and Methods

The highly phosphorylated fraction of rat dentin phosphoprotein (HP) was isolated as described in the preceding paper. All mineral-binding experiments were performed in a total volume of 1.0 mL at an HP concentration of 1.0 mM with respect to organic phosphate (P_o). The total calcium ion concentration was 3.5 or 4.9 mM, and the total inorganic phosphate concentration ranged from 0.20 to 4.0 mM. The pH was 7.4, 8.0, or 8.5, and the ionic strength was 0.028–0.035 or 0.151–0.162 M. At low ionic strength the solutions were buffered with Tris (22.5, 45, and 90 mM at pH 7.4, 8.0, and 8.5, respectively). At high ionic strength the solutions were buffered with 0.126 M NaCl and Tris (22.5 mM at pH 7.4 and 8.0 and 45 mM at pH 8.5). The solutions were doubly labeled at specific activities of about 1.5×10^6 dpm/μmol for ^{45}Ca and about 1.0×10^5 dpm/μmol for ^{32}P. Mineral binding was initiated by adding calcium to solutions containing protein and inorganic phosphate. Within 10 min of mixing, 0.5 mL

† Supported by National Institutes of Health Grant AR-36239.

[1] Abbreviations: HP, highly phosphorylated phosphophoryn; P_o, organic phosphate; ACP, amorphous calcium phosphate; HA, hydroxyapatite; OCP, octacalcium phosphate; TCP, tricalcium phosphate; DCPD, dicalcium phosphate dihydrate; Tris, tris(hydroxymethyl)-aminomethane.

0006-2960/89/0428-0346$01.50/0

of ultrafiltrate was collected by centrifuging the solutions for 5 min at 1000g in Amicon micropartition cells (MPS-1) equipped with YMT membranes. Free calcium and phosphate were determined from the ^{45}Ca and ^{32}P concentration of the ultrafiltrate. Protein-bound calcium and phosphate were determined by the difference in the total and free calcium and phosphate, respectively. The data are expressed as the number of calcium ions ν_{Ca} and phosphate ions ν_P bound to the protein per organic phosphate residue.

The concentration of free calcium and phosphate in contact with amorphous calcium phosphate (ACP) was measured by the same technique but omitting the protein. Here, 2.3 mM calcium was mixed with 0.25–2.5 mM inorganic phosphate at pH 8.0 in 50 mM Tris, and the soluble ions in the ultrafiltrate were measured. The calcium and phosphate concentrations of the solutions and their ultrafiltrates were identical in the absence of precipitation, i.e., when the calcium and phosphate concentrations were too low for the spontaneous precipitation of ACP.

The Ca^{2+} and PO_4^{3-} activities were determined from the free calcium and phosphate concentrations with

$$[P] = (H_3PO_4) + (H_2PO_4^-)/f_1 + (HPO_4^{2-})/f_2 + (PO_4^{3-})/f_3 + (CaH_2PO_4^+)/f_1 + (CaHPO_4) + (CaPO_4^-)/f_1 \quad (1)$$

$$[Ca] = (Ca^{2+})/f_2 + (CaH_2PO_4^+)/f_1 + (CaHPO_4) + (CaPO_4^-)/f_1 + (CaOH^+)/f_1 \quad (2)$$

where [ ] indicates concentrations, ( ) indicates activities, and f_1, f_2, and f_3 are the activity coefficients for singly, doubly, and triply charged ions, respectively. Activity coefficients for uncharged species are assumed to be 1.0. Combining eq 1 and 2, dropping terms involving (H_3PO_4), (PO_4^{3-}), and $(CaOH^+)$ which are small in the pH range examined, and expressing all unknowns as functions of (Ca^{2+}), (PO_4^{3-}), and (H^+) gives

$$(PO_4^{3-}) = \left[\left(\frac{[P]-[Ca]}{2A} - \frac{1}{2f_2B}\right)^2 + \frac{[P]}{ABf_2}\right]^{1/2} + \frac{[P]-[Ca]}{2A} - \frac{1}{2f_2B} \quad (3)$$

and

$$(Ca^{2+}) = \frac{[Ca]f_2}{1 + f_2B(PO_4^{3-})} \quad (4)$$

where

$$A = \frac{(H^+)^2}{f_1K_2K_3} + \frac{(H^+)}{f_2K_3}$$

and

$$B = \frac{(H^+)^2}{f_1K_2K_3K'_3} + \frac{(H^+)}{K_3K'_2} + \frac{1}{f_1K'_1}$$

K_2, K_3, K'_1, K'_2, and K'_3 are the dissociation constants at 25 °C for $H_2PO_4^-$, HPO_4^{2-}, $CaPO_4^-$, $CaHPO_4$, and $CaH_2PO_4^+$, respectively. K_2 and K_3 are taken from Bates and Acree (1943) and Bates (1951), respectively. Values of K'_1, K'_2, and K'_3 are from Chughtai et al. (1968). The activity coefficients were calculated from the Davies (1962) modification of the Debye–Hückel equation:

$$\log \frac{1}{f_i} = 0.5Z_i^2\left(\frac{I^{1/2}}{1 + I^{1/2}} - 0.3I\right) \quad (5)$$

where I is the ionic strength of the medium and Z_i is the charge on ion i. The ionic strength was estimated from

$$I = I_B + \frac{[Cl^-]_{Ca}}{2} + \frac{[Na^+]_P}{2} + \frac{2(Ca^{2+})}{f_2} + \frac{(Ca^{2+})(PO_4^{3-})}{2f_1}\left[\frac{(H^+)^2}{K_2K_3K'_3} + \frac{1}{K'_1}\right] + (PO_4^{3-})\left[\frac{(H^+)^2}{2f_1K_2K_3} + \frac{2(H^+)}{f_2K_3}\right] \quad (6)$$

where I_B is the ionic strength of the buffer, $[Cl^-]_{Ca}$ is the concentration of chloride added as $CaCl_2$, $[Na^+]_P$ is the concentration of Na^+ added as sodium phosphate, and the last five terms represent the ionic strength of Ca^{2+}, $CaH_2PO_4^+$, $CaPO_4^-$, $H_2PO_4^-$, and HPO_4^{2-}, respectively. The concentrations of H^+, OH^-, and PO_4^{3-} are very small and not included in eq 6. The contribution of the protein to the ionic strength was ignored. I_B was determined as the sum of the NaCl concentration and the HCl concentration added to bring the Tris buffer to the required pH. The activity coefficients, (PO_4^{3-}), (Ca^{2+}), and I were calculated with eq 5, 3, 4, and 6, respectively, using successive approximations. For the first iteration I was set equal to I_B. Two to three iterations were required for convergence. An IBM PC25 computer was programed to execute the calculations.

To measure the stability of the calcium phosphate–protein complexes, ^{32}P- and ^{45}Ca-labeled complexes were reequilibrated with a phosphate-free buffer containing unlabeled calcium ions. One milliliter of the labeled protein solution (prepared as described above) was chromatographed on a 0.9 × 100 cm column of Sephadex G-50 equilibrated with 0.7–5.0 mM $CaCl_2$, 140 mM NaCl, and 25 mM Tris, pH 7.4. Undissociated ^{32}P and ^{45}Ca were eluted in the void volume with the protein. No radiolabeled ions eluted in the void volume when control solutions containing no protein were chromatographed under the same conditions. The reequilibration period was varied from 35 to 190 min by using elution rates of 43–9 mL/h, respectively.

Calcium phosphate–protein complexes were deposited on carbon-coated grids as described in the preceding paper and examined with an Hitachi 11E electron microscope. For examination in the imaging mode, the protein was rotary coated with Pt–Pd (80:20) at a 6° angle. Uncoated protein was examined in the diffraction mode. No reflections attributable to a crystalline calcium phosphate phase were observed. All reflections were broad diffuse rings which were attributable to the protein and carbon substrate, since the protein in the absence of inorganic phosphate produced the same diffraction image.

Results

Formation and Analysis of Calcium Phosphate–Protein Complexes. In the presence of calcium ions, rat dentin highly phosphorylated protein (HP) binds inorganic phosphate ions, and the level of binding at constant protein concentration is a function of the pH, ionic strength, and calcium and phosphate concentration of the medium (Figures 1 and 2). At a constant concentration of total calcium (free plus bound), the calcium content of the protein ν_{Ca} increases with the phosphate content ν_P. For the purpose of analyzing the binding curves in Figures 1 and 2, it is convenient to treat the system as if the protein sequesters two different ligands, i.e., calcium ions Ca^{2+} and calcium phosphate clusters Ca_xP. To determine the stoichiometry of Ca_xP, $\nu_{Ca} - \nu^\circ_{Ca}$ is plotted as a function

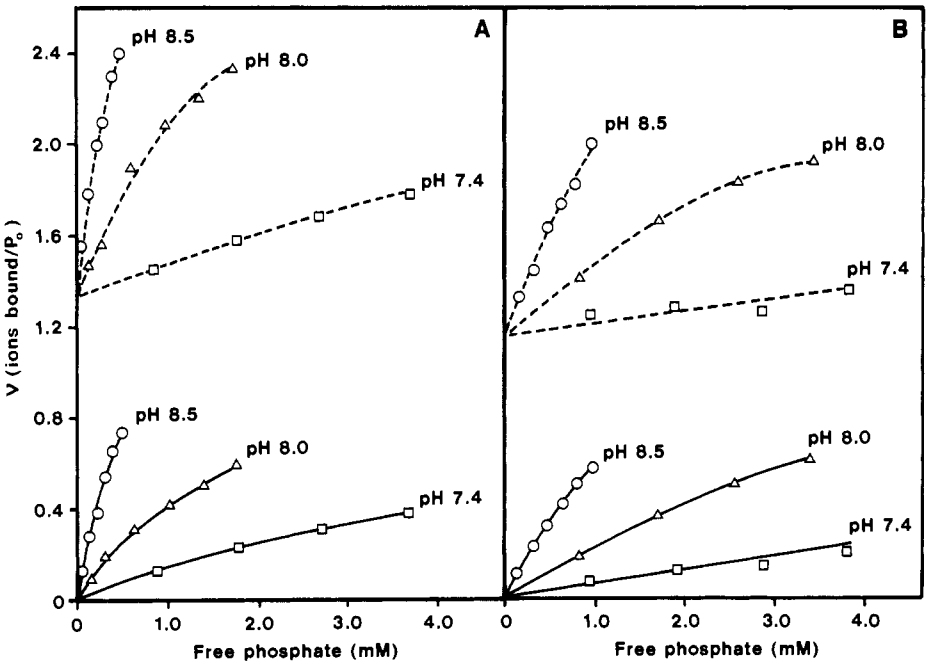

FIGURE 1: Titration of HP (1.0 mM in organic phosphate, P_o) with inorganic phosphate in the presence of 3.5 mM total calcium at pH 7.4 (□), 8.0 (△), and 8.5 (○). Broken lines represent ν_{Ca} (calcium ions bound/P_o), and solid lines represent ν_P (inorganic phosphate ions bound/P_o). (A) Ionic strength 0.028–0.035 M. (B) Ionic strength 0.152–0.162 M.

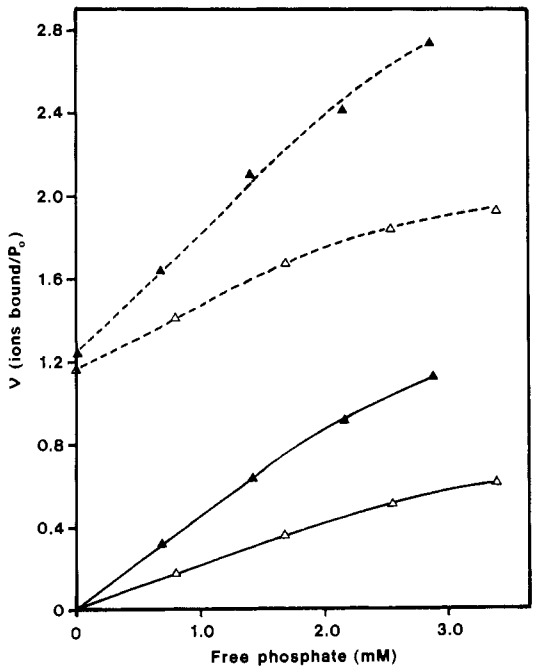

FIGURE 2: Titration of HP (1.0 mM P_o) with inorganic phosphate at pH 8.0, ionic strength 0.152–0.157 M, in the presence of 3.5 (△) and 4.9 mM (▲) total calcium. ν_{Ca} (– –); ν_P (—).

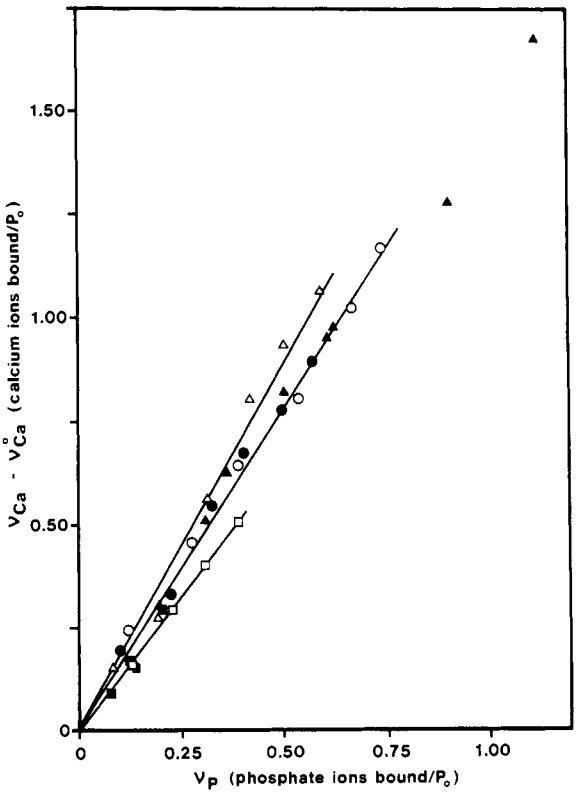

FIGURE 3: Data in Figures 1 and 2 plotted as $\nu_{Ca} - \nu^\circ_{Ca}$ vs ν_P. Ionic strength 0.028–0.035 M and pH 7.4 (□), 8.0 (△), or 8.5 (○). Ionic strength 0.152–0.162 M and pH 7.4 (■), 8.0 (▲) or 8.5 (●). ν°_{Ca} determined as described in the text. Slope ranges from 1.3 to 1.75.

of ν_P (Figure 3), where ν°_{Ca} is the calcium bound under the same conditions but in the absence of phosphate. ν°_{Ca} was determined from the free Ca^{2+} concentration in the system and Figure 3 in the preceding paper, which gives ν°_{Ca} as a function of $[Ca^{2+}]$. $(\nu_{Ca} - \nu^\circ_{Ca})/\nu_P$ ranges from 1.30 to 1.75 depending to some extent upon the conditions. The average stoichiometry of the cluster is about $Ca_{1.5}P$.

ν_P and ν_{Ca} increase as the pH is increased from 7.4 to 8.5 (Figure 1), but ν°_{Ca} remains constant (preceding paper). This suggests that the protein preferentially sequesters multiply charged phosphate ions. If the protein exclusively binds either HPO_4^{2-} or PO_4^{3-}, then $\nu_{Ca} - \nu^\circ_{Ca}$ and ν_P should be a function of the activity product $(Ca^{2+})^{1.5}(HPO_4^{2-})$ or $(Ca^{2+})^{1.5}(PO_4^{3-})$, respectively, and the function should be independent of pH. Activity products as opposed to concentration products are indicated because of the strong dependence of ν_{Ca} and ν_P on ionic strength (Figure 1). Curves describing $\nu_{Ca} - \nu^\circ_{Ca}$ and ν_P as a function of $(Ca^{2+})^{1.5}(PO_4^{3-})$ at different pH are very nearly coincident, at both high and low ionic strength (Figure 4). Curves relating $\nu_{Ca} - \nu^\circ_{Ca}$ and ν_P to $(Ca^{2+})^{1.5}(HPO_4^{2-})$ are quite clearly distinct at different pH, similar to the curves

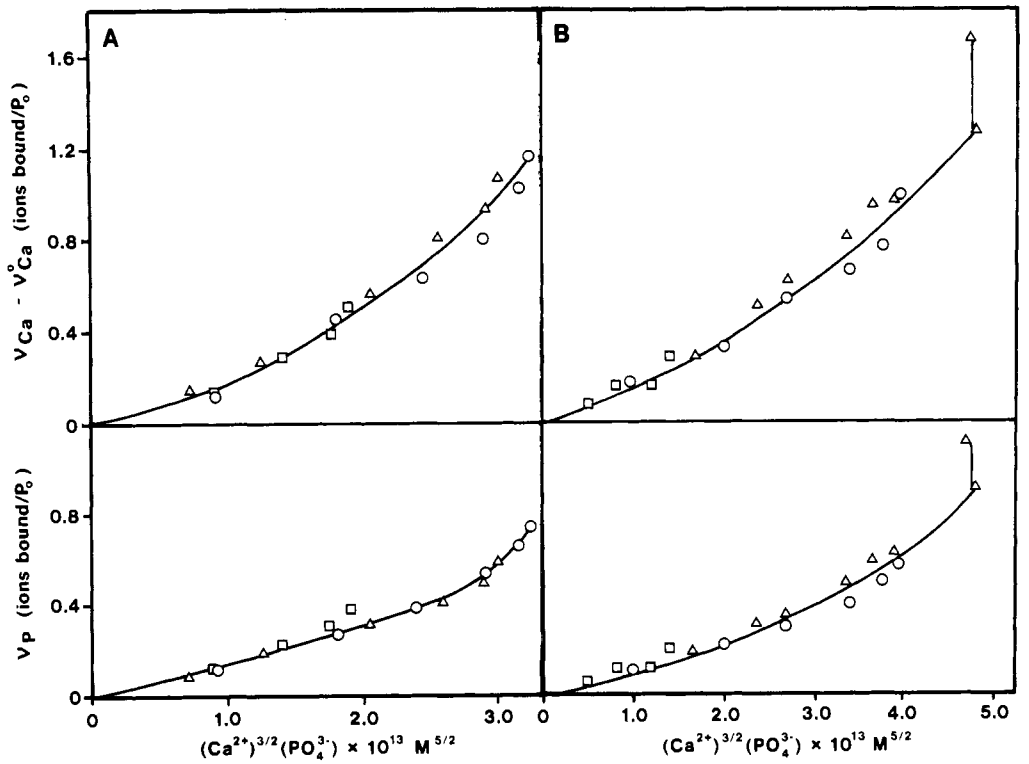

FIGURE 4: $\nu_{Ca} - \nu^{\circ}_{Ca}$ and ν_P plotted as a function of the activity product $(Ca^{2+})^{1.5}(PO_4^{3-})$. Measurements made at pH 7.4 (□), 8.0 (△), and 8.5 (○). (A) Ionic strength 0.028–0.035 M. (B) Ionic strength 0.152–0.162 M.

in Figure 1. Therefore, the protein sequesters PO_4^{3-}, even though (HPO_4^{3-}) is 4–5 orders of magnitude greater than (PO_4^{3-}) in the pH range of 8.5–7.4 and the activity of the ion pair $CaHPO_4$ is 1.7–22 times greater than the activity of $CaPO_4^-$ in the same pH range.

Figure 5 shows the experimentally measured Ca^{2+} and PO_4^{3-} activities of solutions in contact with amorphous calcium phosphate (ACP) and the protein–calcium phosphate complex at pH 8.0 and low ionic strength. The value of ν_P is given for each data point representing solutions containing the protein complex, and the points are connected by a dashed line. The same figure also shows the Ca^{2+} and PO_4^{3-} activities in equilibrium with crystalline calcium phosphates at 25 °C and pH 8.0. The crystalline phases are hydroxyapatite (HA), $Ca_5(OH)(PO_4)_3$; tricalcium phosphate (TCP), $Ca_3(PO_4)_2$; octacalcium phosphate (OCP), $Ca_8H_2(PO_4)_6 \cdot 5H_2O$; and dicalcium phosphate dihydrate (DCPD), $CaHPO_4 \cdot 2H_2O$. These isotherms were constructed with the solubility product constants given by Nancollas (1982). At values of ν_P less than 0.4 ion per organic phosphate residue, the solution in contact with the protein complex is supersaturated with respect to HA, TCP, and OCP (i.e., the points lie above the isotherm lines for the HA, TCP, and OCP phases). At ν_P greater than 0.4, the solution is also supersaturated with respect to DCPD. At ν_P about 0.8, the protein complex curve will intersect the ACP line. Beyond this point protein binding of calcium phosphate is unmeasurable, due to precipitation of ACP. Note the apparent increase in ν_P in Figure 4B at a constant ion product.

The mineral–protein complex is amorphous by electron diffraction analysis, and complexes aged in contact with the solution for 24 h are also amorphous. It has been proposed that ACP is composed of $Ca_9(PO_4)_6$ clusters (Betts et al., 1981). Since $\nu_{Ca} - \nu^{\circ}_{Ca}$ and ν_P can be expressed as a function of $(Ca^{2+})^{1.5}(PO_4^{3-})$, the protein may sequester ACP clusters. The same data cannot be expressed as a pH-invariant function of $(Ca^{2+})^{1.33}(H^+)^{0.33}(PO_4^{3-})$ or $(Ca^{2+})^{1.67}(OH^-)^{0.33}(PO_4^{3-})$ as shown in Figure 6. Therefore, the protein does not sequester

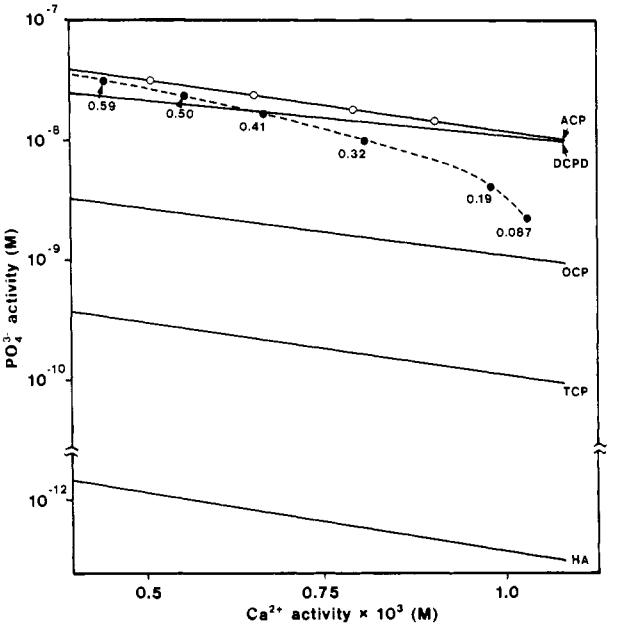

FIGURE 5: log (PO_4^{3-}) vs log (Ca^{2+}) of solutions in equilibrium with HA, TCP, OCP, and DCPD at pH 8.0 calculated from solubility product constants and of solutions in contact with ACP (○) and the protein–mineral ion complex (●) determined experimentally at pH 8.0 and ionic strength 0.031–0.035 M. ν_P is given for each data point representing the protein–mineral ion complex.

crystal embryos of OCP or HA. Empirically, $\nu_{Ca} - \nu^{\circ}_{Ca}$ and ν_P can best be described as a pH-invariant function of a neutral ion activity product in which a small percent of the total phosphate is HPO_4^{2-}. These data are not shown because the curves are very similar to those in Figure 4. The only significant difference is that almost every data point falls on the curves. The best stoichiometry for the sequestered clusters is $Ca_{1.48}(HPO_4)_{0.025}(PO_4)_{0.975}$ at low ionic strength and $Ca_{1.45}(HPO_4)_{0.10}(PO_4)_{0.90}$ at high ionic strength.

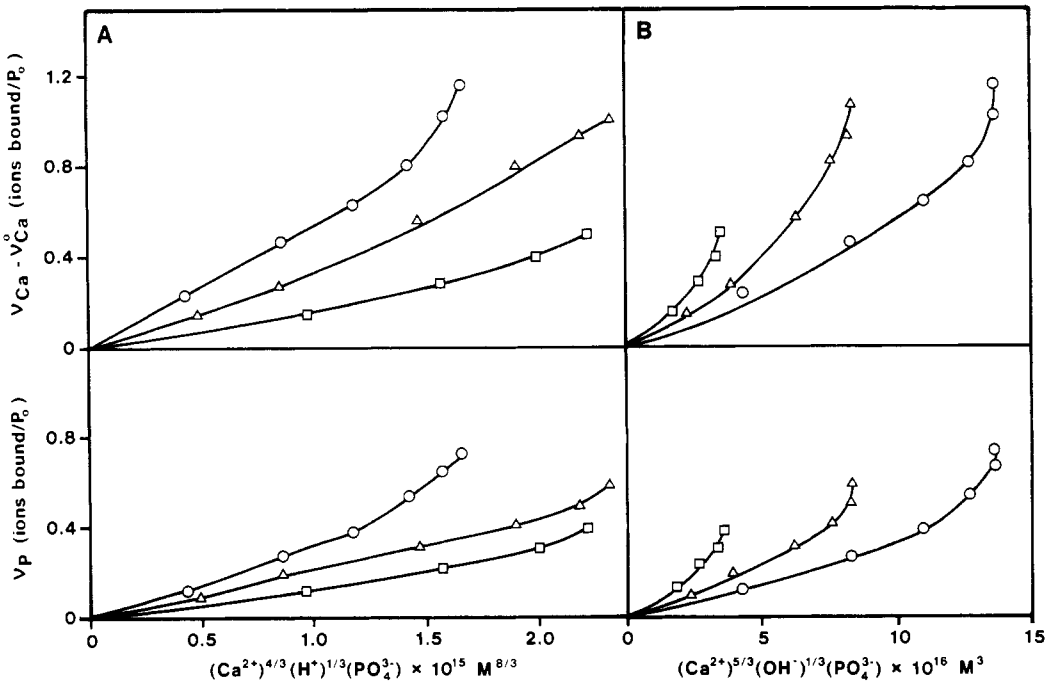

FIGURE 6: $\nu_{Ca} - \nu^{\circ}_{Ca}$ and ν_P plotted as a function of the activity products $(Ca^{2+})^{1.33}(H^+)^{0.33}(PO_4^{3-})$ and $(Ca^{2+})^{1.67}(OH^-)^{0.33}(PO_4^{3-})$ in (A) and (B), respectively, at pH 7.4 (□), 8.0 (△), and 8.5 (○). Data are shown for ionic strength 0.028–0.035 M; curves for ionic strength 0.152–0.162 M are similar.

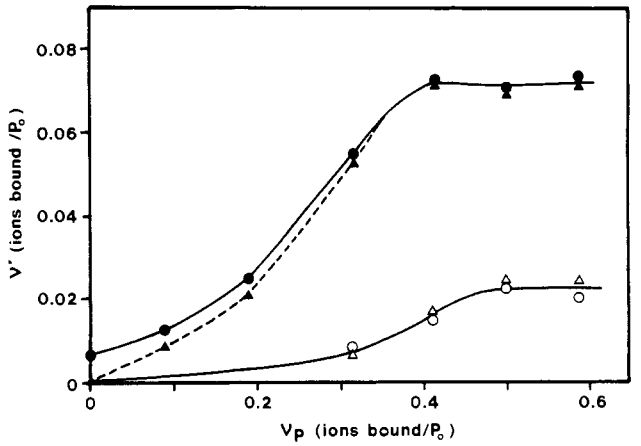

FIGURE 7: ν'_{Ca} (○, ●) and ν'_P (△, ▲) plotted as a function of ν_P. ν'_{Ca} and ν'_P were measured after equilibration for 35 min in a phosphate-free buffer containing 0.7 (○, △) and 2.0 mM (●, ▲) calcium at pH 7.4 and ionic strength about 0.175 M.

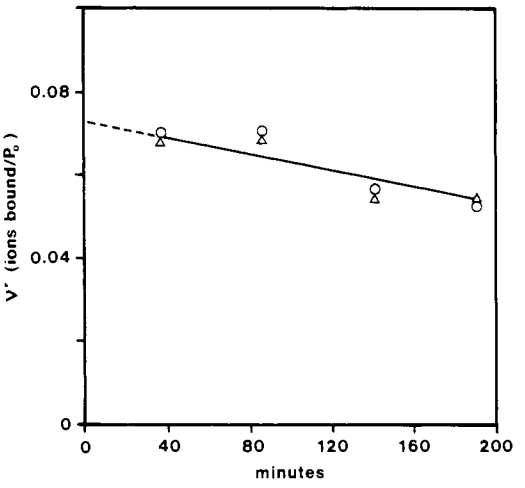

FIGURE 8: ν'_{Ca} (○) and ν'_P (△) plotted as a function of time in a phosphate-free buffer containing 2.0 mM calcium at pH 7.4 and ionic strength about 0.175 M.

Stability of Calcium Phosphate–Protein Complexes. ^{32}P- and ^{45}Ca-labeled protein–mineral complexes were reequilibrated via molecular sieve chromatography with phosphate-free solutions containing 0.70–5.0 mM Ca^{2+} (unlabeled) at pH 7.4 and high ionic strength in order to measure nondissociable (or slowly dissociable) calcium and phosphate, ν'_{Ca} and ν'_P, respectively. Dissociable calcium is replaced with unlabeled calcium to the extent determined by the pH, ionic strength, and Ca^{2+} concentration of the medium, but all dissociable phosphate is lost. Figure 7 describes ν'_{Ca} and ν'_P as a function of ν_P after 35 min of reequilibration. The nondissociable ion binding sites saturate when ν_P reaches about 0.4 ion per organic phosphate residue. The maximum value of ν'_{Ca} and ν'_P is determined by the free calcium concentration in the medium. When free calcium is 0.7 mM, the protein is 50% saturated with Ca^{2+} (Figure 3, previous paper), and the ν'_P maximum is 0.022. The ν'_P maximum is 0.070 at calcium concentrations of both 2.0 (Figure 7) and 5.0 mM (data not shown), where the protein is 83 and 100% saturated with Ca^{2+}, respectively. ν'_P ranges from $0.05\nu_P$ to $0.15\nu_P$, and at saturation $\nu'_P = \nu'_{Ca}$. The nondissociable ions are stable for extended periods in the absence of free phosphate, as shown in Figure 8 which describes ν'_{Ca} and ν'_P as a function of time in a phosphate-free calcium buffer.

The experiments summarized here give no information on the ionization state of P or the stoichiometry of the Ca_xP complexes in the protected domains (i.e., nondissociable calcium and phosphate), because the bound ligands are not in equilibrium with the free ligands. $\nu'_{Ca} = \nu'_P$ at saturation does not imply the presence of CaP complexes. Some domains may sequester protected Ca^{2+} and others protected Ca_xP. Alternatively, some domains sequestering protected Ca_xP may have large enough openings to permit the free exchange of Ca^{2+}, but not large enough to permit the free diffusion of the larger ^{32}P ions.

Once the protected domains are charged with calcium and phosphate, the protein remains in an aggregated state even in phosphate-free buffers having a calcium ion concentration

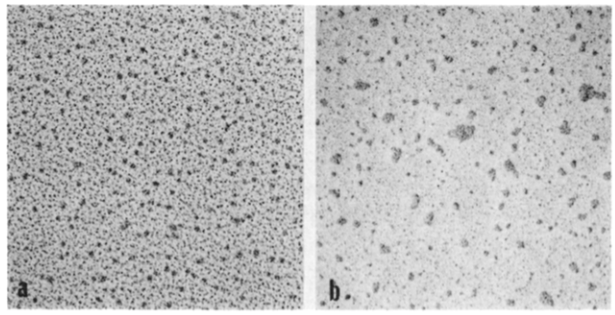

FIGURE 9: Electron micrographs of HP equilibrated with 2.0 mM calcium at pH 7.4 and ionic strength 0.175 M. Magnification 42000×. (a) Free protein. (b) Mineralized protein containing 0.07 calcium and inorganic phosphate ions (per organic phosphate residue) in protected domains.

too low to support free protein aggregation. Figure 9a shows an electron micrograph of the free protein equilibrated with 2.0 mM Ca^{2+} at pH 7.4 and ionic strength about 0.175 M. Figure 9b shows the mineralized protein equilibrated with the same buffer. It appears that only the aggregated protein sequesters protected calcium phosphate.

Discussion

The amount of phosphate sequestered by rat dentin HP is a function of the activity product $(Ca^{2+})^{1.5}(PO_4^{3-})$ of the medium. The experimental data are actually not good enough to determine the power of the calcium dependence. For each PO_4^{3-} bound, the protein sequesters 1.3–1.75 additional Ca^{2+} ions. This range of values was determined from the difference in bound calcium ($\nu_{Ca} - \nu^{\circ}_{Ca}$) in the presence and absence of PO_4^{3-} under the same conditions. This approximation assumes that the binding of Ca^{2+} ions is independent of the amount of calcium phosphate associated with the protein, i.e., that $\nu_{Ca} = g[(Ca^{2+})] + g'[(Ca^{2+})^x(PO_4^{3-})]$, where g and g' are two distinct and additive functions and x is the ratio of Ca/PO_4 in the cluster. Since $\nu_{Ca} - \nu^{\circ}_{Ca}$ and ν_P are well fitted to a function of $(Ca^{2+})^{1.5}(PO_4^{3-})$, it is likely that variation in x is due largely to experimental error. ν_{Ca}, ν°_{Ca}, and ν_P are each determined by the difference of two measurements, so the value of x which is $(\nu_{Ca} - \nu^{\circ}_{Ca})/\nu_P$ involves six independent measurements. The observed range of x (1.3–1.75) differs from the average value (about 1.5) by no more than 14%. There is also a theoretical basis for x having a value of 1.5. The affinity and capacity of the protein for Ca^{2+} is based on the electrostatic charge on the protein. Therefore, the binding of Ca^{2+} will be independent of sequestered Ca_xPO_4 only if the complex is neutral; i.e., $Ca/PO_4 = 1.5$.

Although there is a degree of uncertainty in the Ca/PO_4 ratio, there is little uncertainty in the ionization state of the bound phosphate, because the binding experiments were performed over a pH range of 7.4–8.5. When ν_P is measured as a function of the phosphate concentration at only one pH, it is impossible to determine which phosphate ion is the ligand, because although the total free phosphate increases during the titration, the ratio of $(PO_4^{3-})/(HPO_4^{2-})$ remains constant. But when the pH is varied from 7.4 to 8.5, there is a 1260% increase in the PO_4^{3-} activity relative to the HPO_4^{2-} activity, and then it is apparent that ν_P is a function of (PO_4^{3-}) and not (HPO_4^{2-}). Note that from the preceding paper there is no observable change in the ionization state of the organic phosphate residues in the protein above pH 7.4, so that all variation in ν_P with pH can be attributed to the altered ionization state of the inorganic phosphate ion. It is also clear that the protein does not bind ion clusters which could be considered HA or OCP embryos. The former has a stoichiometry of $Ca_{1.67}(OH)_{0.33}(PO_4)$ and the latter $Ca_{1.33}H_{0.33}(PO_4)$. It is not possible to eliminate HA or OCP cluster binding on the basis of the Ca/P ratio of the bound mineral, since the experimental values range from 1.3 to 1.75. However, it is easy to rule out the dependence of ν_P on (OH^-) and (H^+) by curve fitting (Figure 6). Again, it is apparent that the pH influences ν_P only by effecting the ionization state of P.

Since ν_P is a function of $(Ca^{2+})^{1.5}(PO_4^{3-})$, it is also a function of $(Ca^{2+})^{1.5n}(PO_4^{3-})^n$. It is not possible to determine whether the protein binds preformed clusters $Ca_{1.5n}(PO_4)_n$, where n is a positive even number, or a collection of individual ions and simple ion pairs which taken together have a stoichiometry of $Ca_{1.5}PO_4$. However, it is significant that the binding data are best fitted to an ion activity product function in which 2.5–10% of the PO_4^{3-} is replaced by HPO_4^{2-}. Using an analogous method, Meyer and Eanes (1978) found that the ion activity product of solutions in contact with ACP are invariant to pH if the mineral phase has a HPO_4^{2-}/PO_4^{3-} ratio of about 0.10. Since the mineral cluster bound to the protein is compositionally similar to ACP, it is probable that the protein sequesters preformed ACP clusters or that ACP clusters form on the protein. For values of ν_P less than 0.4, the solution in contact with the protein–mineral complex is supersaturated with respect to OCP but undersaturated with respect to DCPD (Figure 5). Under these conditions, OCP precipitates directly from solution without the formation of an ACP precursor phase in the presence of a suitable seeding agent (Koutsoukos et al., 1980). Although phosphophoryn is not a nucleator of OCP, it might be expected that the protein would sequester OCP-like clusters. However, this is clearly not the case because curves describing ν_P as a function of $(Ca^{2+})^{1.33}(H^+)^{0.33}(PO_4^{3-})$ are not invariant to pH (Figure 6A). One possible explanation is that only ACP-like clusters form in solution, and the clusters hydrolyze to OCP concurrently with precipitation when solutions are supersaturated with respect to OCP and undersaturated with respect to DCPD. Another possible explanation is that the calcium and phosphate ion activities are considerably higher in the vicinity of a polyanion than in the solution as a whole (Crenshaw, 1982); here the protein may be in local contact with a solution which is supersaturated with respect to DCPD, while the bulk solution is undersaturated with respect to DCPD. Either one of these scenarios would explain the sequestration of ACP-like clusters by phosphophoryn.

Although phosphophoryn can sequester mineral ion clusters, it does not promote the conversion of sequested mineral to crystalline HA under the conditions examined here, even though the majority of the sequestered ions are exposed to the solution. In a preliminary study, Lussi et al. (1988) observed that phosphophoryn covalently attached to agarose beads catalyzed the crystallization of HA from metastable solutions of calcium phosphate. The significant difference in these two systems is that immobilized phosphophoryn cannot self-associate in the presence of calcium and phosphate. The surface of the immobilized monomer may be quite different from the aggregate surface.

Up to 15% of the calcium phosphate sequestered by HP is buried in protected domains, and it is stable for extended periods in the presence of phosphate-free calcium buffers. The buried mineral maintains the protein in an aggregated state even at calcium ion concentrations which are too low for the aggregation of unmineralized HP. If phosphophoryn is secreted into the extracellular environment in a mineralized aggregated state similar to casein and the bivalve phosphoprotein, it cannot catalyze either the direct nucleation of a

crystalline phase or the conversion of amorphous calcium phosphate to hydroxyapatite. However, the aggregate does provide a locally high concentration of bound mineral ions, so that degradation of the protein would lead to spontaneous precipitation of a mineral phase or to growth of preexisting mineral. Alternatively, if phosphophoryn is secreted as a monomer and immobilized on the collagen fibrils in the dentin matrix before aggregation can occur, then conceivably the protein could catalyze the formation of hydroxyapatite crystals. In vitro studies alone do not give enough information to define the role of high-capacity calcium-binding proteins in the mineralization process. Intracellular pathways for phosphophoryn mineralization and aggregation must also be examined.

ACKNOWLEDGMENTS

I am grateful to Sam Marsh for writing the program to calculate mineral ion activities.

REFERENCES

Bates, R. G. (1951) *J. Res. Natl. Bur. Stand. (U.S.) 47*, 127-134.
Bates, R. G., & Acree, S. F. (1943) *J. Res. Natl. Bur. Stand. (U.S.) 30*, 129-155.
Betts, F., Blumenthal, N. C., & Posner, A. S. (1981) *J. Cryst. Growth 53*, 63-73.
Chughtai, A., Marshall, R., & Nancollas, G. H. (1968) *J. Phys. Chem. 72*, 208-211.
Crenshaw, M. A. (1982) in *Biological Mineralization and Demineralization* (Nancollas, G. H., Ed.) pp 243-258, Springer-Verlag, New York.
Davies, C. W. (1962) *Ion Association*, Butterworth, London.
Dimuzio, M. T., & Veis, A. (1978) *J. Biol. Chem. 253*, 6845-6852.
Glimcher, M. J. (1981) in *The Chemistry and Biology of Mineralized Tissues* (Veis, A., Ed.) pp 618-673, Elsevier, New York.
Holt, C. (1982) *J. Dairy Res. 49*, 29-38.
Koutsoukos, P., Amjad, Z., Tomson, M. B., & Nancollas, G. H. (1980) *J. Am. Chem. Soc. 102*, 1553-1557.
Lee, S. L., Veis, A., & Glonek, T. (1977) *Biochemistry 16*, 2971-2979.
Lee, S. L., Glonek, T., & Glimcher, M. J. (1983) *Calcif. Tissue Int. 35*, 815-818.
Linde, A., Bhown, M., & Butler, W. T. (1980) *J. Biol. Chem. 255*, 5931-5942.
Lussi, A., Crenshaw, M. A., & Linde, A. (1988) *J. Dent. Res. 67*, 180.
Maier, G. D., Lechner, J. H., & Veis, A. (1983) *J. Biol. Chem. 258*, 1450-1455.
Marsh, M. E. (1988) in *Origin, Evolution and Modern Aspects of Biomineralization in Plants and Animals* (Crick, R. E., Ed.) Plenum, New York (in press).
Marsh, M. E., & Sass, R. L. (1984) *Biochemistry 23*, 1448-1456.
Meyer, J. L., & Eanes, E. D. (1978) *Calcif. Tissue Res. 25*, 59-68.
Nancollas, G. H. (1982) in *Biological Mineralization and Demineralization* (Nancollas, G. H., Ed.) pp 79-99, Springer-Verlag, New York.
Nawrot, C. F., Campbell, D. J., Schroeder, J. K., & Van Valkenburg, M. (1976) *Biochemistry 15*, 3445-3449.
Termine, J. D., & Conn, K. M. (1976) *Calcif. Tissue Res. 22*, 149-157.
Termine, J. D., Eanes, E. D., & Conn, K. M. (1980) *Calcif. Tissue Int. 31*, 247-251.
Veis, A. (1978) *Colston Pap. 29*, 259-272.

Analysis of Peptides for Helical Prediction†

Gene Merutka and Earle Stellwagen*
Department of Biochemistry, University of Iowa, Iowa City, Iowa 52242
Received March 22, 1988; Revised Manuscript Received July 12, 1988

ABSTRACT: Two terminally blocked peptides, acetylAETAAAKFLRQHMamide and acetyl-AETSSSRYLRQHMamide, were obtained by solid-phase synthesis, purified by reversed-phase chromatography, and characterized by fast atom bombardment mass spectrometry. Both peptides were soluble in aqueous solutions and remained monomeric over the concentration range examined. Changes in the temperature, pH, and trifluoroethanol concentration of solutions of each peptide produced changes in the far-ultraviolet circular dichroic spectrum characteristic of a two-state helix/coil transition. The limiting mean residue ellipticity of the coil and helix form of each peptide was estimated by addition of the denaturant guanidinium chloride at elevated temperature and by addition of trifluoroethanol at subzero temperatures, respectively. The midpoint for the thermal transition of the peptide SSSRY is lowered by about 30 °C relative to that of peptide AAAKF, in qualitative agreement from predictions based on helix probabilities of amino acid residues. The magnitude of the change observed in the midpoint of the thermal transitions suggests that the effect of single amino acid replacements on helix formation should be experimentally measurable.

An essential feature of the prediction of the biofunctional structure of a protein from its sequence is the accurate location of the secondary structural elements, the helices, strands, and reverse turns. Unfortunately, the confidence level in the prediction of secondary structural elements using current schemes is not very high, the best efforts being about 70% accurate. One major source of this poor performance may be the statistical values for the occurrence of each amino acid in a given secondary structure based on detailed analyses of

†This investigation was supported by U.S. Public Health Service Program Project Grant HL14388 from the National Heart, Lung and Blood Institute and by National Science Foundation Biological Instrumentation Program Grant DMB 8413658.

0006-2960/89/0428-0352$01.50/0